The Effect of the Intake Port Configuration on the Flow and Combustion in a 4-Valve Pentroof Gasoline Engine

Jeongmin Lee, Hongsuk Kim*
Graduate School of Mechanical Engineering, Sungkyunkwan University
Nakwon Sung
School of Mechanical Engineering, Sungkyunkwan University

The flow field in a cylinder of a 4-valve pentroof engine is studied using the KIVA-3V code. Turbulence is generated from the jet flow through valves and broken down to the small scale eddies in the compression process. It is known that the tumble effectively keeps turbulence during the compression process. In the combustion process, turbulence is known to enhance flame speed by increasing mass, momentum and heat transfer rates. The effects of the intake port angles on the flow and combustion characteristics are studied in this study. To study the effect of turbulence on the combustion process, Cantore combustion model is applied in this study.

Key Words : Tumble Flow, Turbulence, Intake Port Angle, Pentroof Engine, Combustion Model

Nomenclature

A, B, C	: Constant
c_p	: Specific heat at constant pressure
D	: Damping factor
EVC	: Exhaust valve closing
EVO	: Exhaust valve opening
IVC	: Intake valve closing
IVO	: Intake valve opening
m	: Mass
N	: Revolution per minute
n	: Polytropic index
R_c	: Reaction rate of chemical kinetics
R_τ	: Reaction rate of mixing control
R_t	: Crankshaft angular rotational speed
t	: Time
S	: Strain rate
s	: Stoichiometric molar ratio of oxidant to fuel
T	: Temperature
$\boldsymbol{u}$	: Gas velocity vector
u'	: Turbulence intensity
W	: Molecular weight

Greek Symbols

ε	: Turbulent kinetic energy dissipation rate
η	: Ratio of turbulent to mean strain time scale
k	: Turbulent kinetic energy
ρ	: Density
σ	: Viscous stress tensor
τ	: Characteristic turbulent time scale
μ	: Absolute viscosity
ω	: Angular velocity
$\dot{w}_r$	: Global reaction rate

Subscripts

c	: Center of the volume of the combustion chamber
f	: Fuel
fr	: Forward reaction
i	: Denote initiation or cell index
o	: Oxygen
pr	: Product

* Corresponding Author,
E-mail : hongsuk@nature.skku.ac.kr
TEL : +82-31-290-7498 ; **FAX** : +82-31-295-1937
Graduate School of Mechanical Engineering, Sungkyunkwan University, Kyungki-do 440-746, Korea.
(Manuscript **Received** April 25, 2000; **Revised** November 8, 2000)

t : Turbulence

Superscripts

$\cdot$: Time rate of change

1. Introduction

The fluid motion inside a cylinder governs the combustion process and consequently determines exhaust emissions in a spark-ignition engine. Since the flow field is generated during the intake process and transformed during the compression process, a good understanding of the fluid motion during the intake and compression processes is important to improve combustion. In recent years, many researchers have tried to improve the engine efficiencies by lean burn technique. The lean burn engine, though advantageous for the fuel economy, requires additional technique for stable combustion. To stabilize combustion, the flow inside a cylinder should be optimized, and turbulence in the flow should be increased. Since the turbulence enhance the mass, momentum and heat transfer rate, the flame speed is increased and combustion is stabilized. Turbulence is mainly generated in the intake process and easily dissipated during the compression process. (Kang et al; 1994, Kang & Baek; 1996)

In a lean burn engine, the intake ports, intake valves and piston bowl should be designed carefully to generate enough turbulence for combustion. A 4-valve engine can generate high power output because of the high volumetric efficiency. Henlot et al. (1989) found that the principal flow pattern in a 4-valve engine was not the swirl flow, but the tumble flow. Naitoh (1990) who conducted a numerical study on the flow inside a cylinder concluded that tumble flow formed during the intake process was compressed by the piston and eventually broken down to the small scale turbulent eddies at the end of the compression process.

The objective of the present study is to conduct in-cylinder flow analysis for a 4-valve pentroof engine having different intake port angles. The flow field is examined during intake, compression and combustion processes. In this study, the KIVA-3V code (Amsden; 1997) is used for the flow analysis and the combustion model proposed by Cantore et al. (1995) is applied to evaluate the effect of the flow field and turbulence.

Table 1 Specifications of the engine

Bore×Stroke (mm)	86.0×86.0
Connecting Rod Length(mm)	150
Compression Ratio	9.2 : 1
Displacement(cc)	1998
Valve Lift(mm)	9
Engine Speed (rpm)	2000
Valve Timing	IVO BTDC 10° IVC ABDC 55° EVO BBDC 55° EVC ATDC 10°
Intake Pressure (bar)	0.49

2. Numerical Calculation

For this study, a 4 valve pentroof S. I. engine was selected. The specifications of the engine and its operating conditions are listed in Table 1. Figure 1 shows the shapes of meshes for a cylinder. Two types of meshes are used in this study to save computing time. The mesh in Fig. 1(a) is composed of the cylinder head, poppet valves and intake ports for the calculation of a intake process, and the mesh shown in Fig. 1(b) is used for the calculation of combustion and expansion processes. The mesh in Fig. 1(a) has about 28,800 cells at the BDC position of a piston, and the number of cells is reduced to about 10,000 at TDC. When a piston moves upwards, the cells under the piston surface are removed, and when the piston moves downwards, the new cells are created. The mesh in Fig. 1(b) has about 30,900 cells at BDC, and the number of cells is changed about 10,000 at TDC.

2.1 Turbulence model

To calculate turbulent flow fields, the RNG (Renormalization Group) $k-\varepsilon$ model is used. Two transport equations are solved for the turbu-

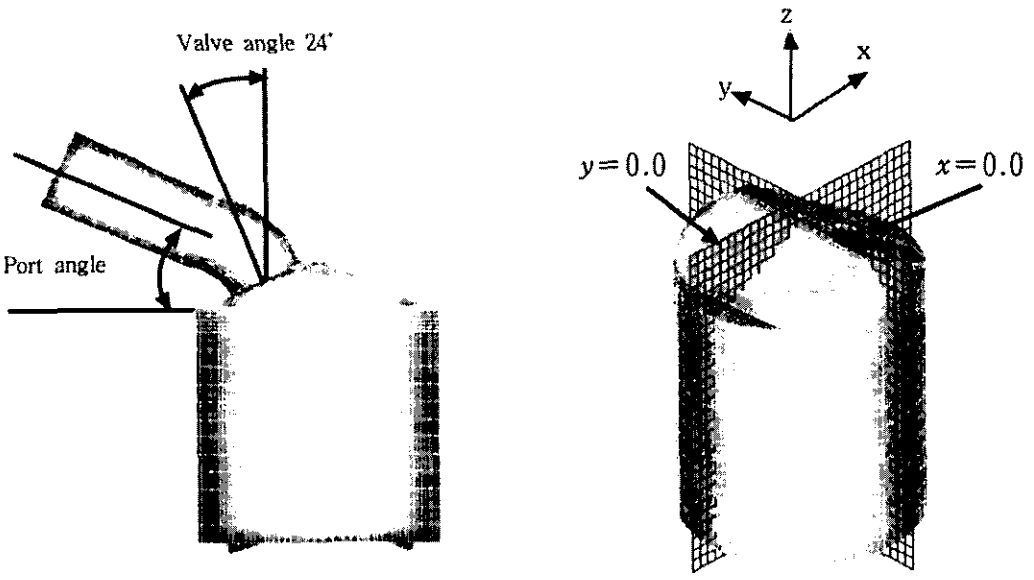

(a) Mesh for calculation of intake process

(b) Mesh for calculation of combustion and expansion process

Fig. 1 Meshes for numerical calculation

lent kinetic energy k and its dissipation rate ε.

$$\frac{\partial \rho k}{\partial t}+\nabla\cdot(\rho \boldsymbol{u}k)=-\frac{2}{3}\rho k\nabla\cdot\boldsymbol{u}+\sigma:\nabla\boldsymbol{u}+\nabla\cdot\left[\left(\frac{\mu}{\mathrm{Pr}_k}\right)\nabla k\right]-\rho\varepsilon \tag{1}$$

$$\frac{\partial \rho \varepsilon}{\partial t}+\nabla\cdot(\rho \boldsymbol{u}\varepsilon)=-\left(\frac{2}{3}C_1-C_3\right)+\frac{2}{3}C_\mu C_\eta\frac{k}{\varepsilon}\nabla\cdot\boldsymbol{u}\rho\varepsilon\nabla\cdot\boldsymbol{u}+\nabla\cdot\left[\left(\frac{\mu}{\mathrm{Pr}_\varepsilon}\right)\nabla\varepsilon\right]+\frac{\varepsilon}{k}[(C_{\varepsilon_1}-C_\eta)\sigma:\nabla u-C_{\varepsilon_2}\rho\varepsilon] \tag{2}$$

where

$$C_3=\frac{-1+C_1-3m(n-1)+(-1)\sqrt[n]{6}C_\mu C_\eta\eta}{3} \tag{3}$$

$$C_\eta=\frac{\eta(1-\eta/\eta_0)}{1+\beta\eta^3} \tag{4}$$

$$\eta=S\frac{k}{\varepsilon} \tag{5}$$

In Eq. (3), constant m is 0.5. $n=1.4$ is used as a polytropic index. η is a ratio of turbulent to mean strain time scale. In Eq. (5), the magnitude of the mean strain is

$$S=(2S_{ij}S_{ij})^{0.5} \tag{6}$$

and,

Table 2 Constants in the turbulence model

C_μ	C_1	C_2	C_3	Pr_k	Pr_ε	η_0	β	C_s
0.085	1.42	1.68	Eq.(10)	0.72	0.72	4.38	0.012	1.5

$$S_{ij}=(\partial\bar{u}_i/\partial x_j+\partial\bar{u}_j/\partial x_i)/2 \tag{7}$$

Values of the constants are listed in Table 2.

2.2 Ignition and combustion models

The ignition was done by adding energy in the cells of the spark kernel during the ignition period (Amsden; 1989). For combustion of fuel, a single step chemical reaction is used. This approach is reasonable to calculate heat release rate and burned mass of fuel in the combustion process(Jennings; 1992). Gasoline is represented by C_8H_{17}.

$$4C_8H_{17}+49O_2+182.28N_2\overset{k_f r}{\Longrightarrow}34H_2O+32CO_2+182.28N_2 \tag{8}$$

The combustion model suggested by Cantore (1995) was used in this study. In the combustion model, reaction rate is calculated with a following procedure. When the temperature in a local cell is high enough or the characteristic time of the

turbulent mixing is much larger than that of the chemical reaction, the flame propagation process is controlled by the turbulent mixing process. The reaction rate R_τ in the turbulent mixing process is calculated by the eddy dissipation model developed by Magnussen et al. (1976).

$$R_\tau = A\left(\frac{\varepsilon}{\chi}\right)\min\left((\rho_f/W_f),\ \frac{(\rho_o/W_o)}{s},\ B\frac{(\rho_{pr}/W_{pr})}{1+s}\right) \tag{9}$$

where A, B are model constants, s is the stoichiometric molar ratio of oxidant to fuel. ρ_o, ρ_f, ρ_{pr} represent the density of oxygen, fuel, and product respectively. W_o, W_f, W_{pr} mean the molecular weight of oxygen, fuel, and product, respectively.

When the temperature in a local cell is low, especially in the vicinity of the cylinder wall and the characteristic time of the chemical reaction is larger than that of the turbulent mixing, the flame propagation is controlled by a chemical reaction process. The reaction rate R_c in the chemical kinetics is given by an Arrhenius-like equation of the form:

$$R_c = \min\left((\rho_f/W_f),\ \frac{(\rho_o/W_o)}{s},\ B\frac{(\rho_{pr}/W_{pr})}{1+s}\right)\beta \cdot \exp\left(-\frac{\delta}{T}\right) \tag{10}$$

where β, δ are constants and T is a temperature of a local cell.

The overall reaction rate $\dot{\omega}_r$ is determined from the small value of the two reaction rates.

$$\dot{\omega}_r = \min(R_\tau,\ R_c) \tag{11}$$

To simulate slow reaction near the wall regions, damping factor D is used to reduce the reaction rate in the cell near the wall(Jennings; 1992).

$$\dot{\omega}_r = D\min(R_\tau,\ R_c) \tag{12}$$

The model constants were selected to match the experimental measurements. The values of the constants are listed in Table 3.

Table 3 Constants in the combustion model

A	B	β	δ	D
43	0.5	6.0×10^5	3000	0.5

2.3 Tumble ratio

Tumble ratio, R_t is defined as the angular velocity of the rotating flow as a solid body, divided by the crankshaft angular rotational speed

$$R_t = \frac{\omega_t}{2\pi N/60} \tag{14}$$

where the angular velocity on the xz plane is given by

$$\omega_t = \frac{\sum_i m_i\{(z_i - z_c)u_i - (x_i - x_c)w_i\}}{\sum_i m_i\{(x_i - x_c)^2 + (z_i - z_c)^2\}} \tag{15}$$

u and w mean the velocity components of x and z direction respectively. The subscript i designates each individual cell, and c designates the center of the volume of the combustion chamber. Point c varies with the volume change, and w_i is velocity component in the z direction. m_i is the mass of the individual cell i.

2.4 Initial and boundary conditions

At the entrance of the intake port, pressure was 0.49 bar, and the temperature of the cylinder wall was 400 K. For initial conditions for a combustion chamber, temperature was 289 K and the pressure was 0.49 bar. Initial time step at the beginning of calculation was 0.1 msec and varied by its time logic, in which the time steps are calculated by the stability criteria. The working fluid was the stoichiometric mixture of C_8H_{17} and air. The engine speed and spark time was fixed at 2000 rpm and 29° BTDC.

2.5 Calculation procedures

The flow field was calculated from the beginning of the intake process to the compression process. The results from the compression process were transferred to the combustion process, using the interpolating technique of Tecplot 7.5. This procedure could reduce the calculation time by reducing cells of ports and valves that are not required in the combustion. The KIVA-3V code was run by a 500MHz Pentium PC having Windows 95/NT. Double precision was kept during the entire calculations. As a FORTRAN compiler, Microsoft FORTRAN Power Station 6.

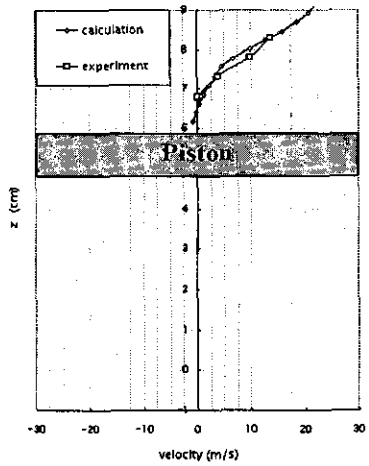

(a) 60° ATDC (intake process)

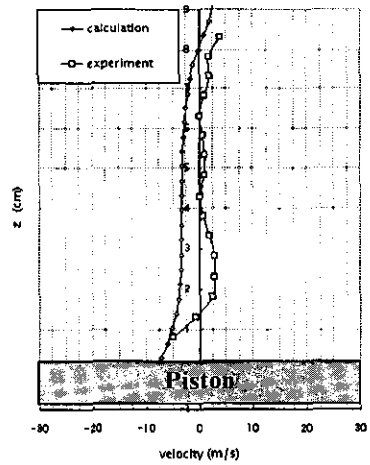

(b) BDC (intake process)

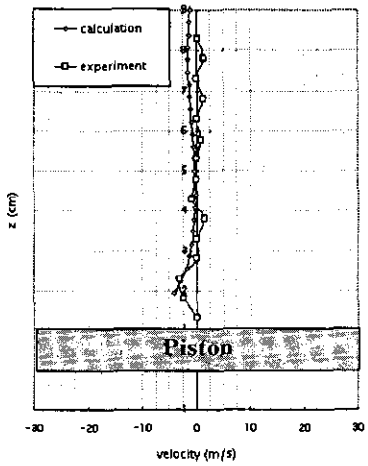

(c) 60° ABDC (compression process)

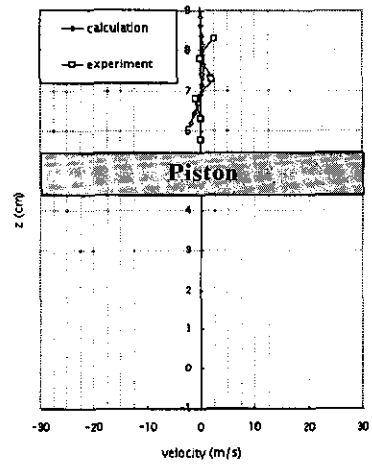

(d) 60° BTDC (compression process)

Fig. 2 Radial velocity variations during the intake and compression processes (at y=0.0 cm plane along the z-axis)

0 was used.

3. Results and Discussions

Figure 2 shows the calculated radial velocity with the experimental measurements. (Kang & Baek; 1996) When the intake valves are opened, the radial flow is formed in the cylinder. As the piston moves downwards, the radial flow is decreasing with the reduced mass flow. In Fig. 2, the calculated results showed good agreement with the experimental measurements.

3.1 The flow field

Figure 3 shows the flow field during the intake and compression processes for 25° port. The flow field is formed by the jet flow from the intake valves. The annular flow through valves is divided into two main jet flows. One strong jet is directed tangent to the combustion chamber and then deflected by the cylinder wall and generates weak counterclockwise tumble. As the piston moves downwards, the strong clockwise tumble dominates in the entire cylinder. At BDC, the strong clockwise tumble is weakened and divided into two medium size tumbles. As the compres-

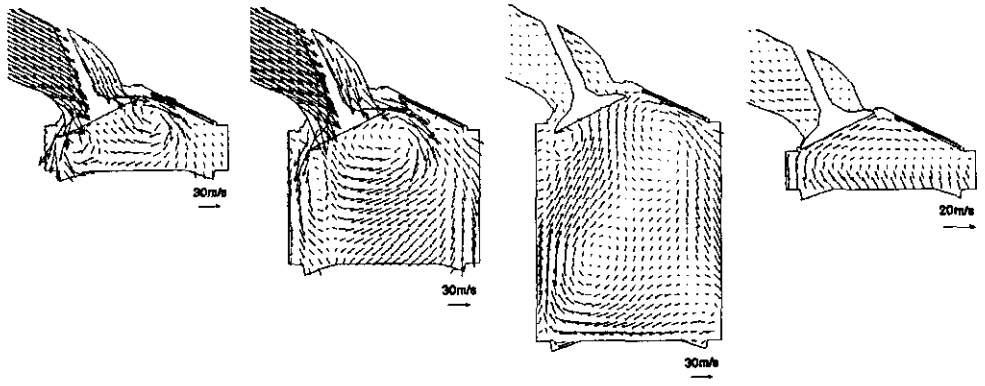

(a) 45° ATDC (a) 90° ATDC (a) BDC (a) 40° BTDC

Fig. 3 Development of flow field during the intake and compression processes (for 25° port)

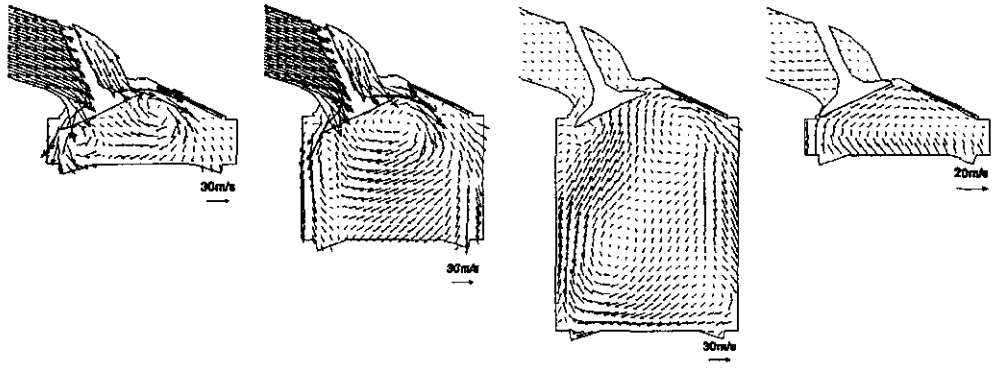

(a) 45° ATDC (a) 90° ATDC (a) BDC (a) 40° BTDC

Fig. 4 Development of flow field during the intake and compression processes (for 15° port)

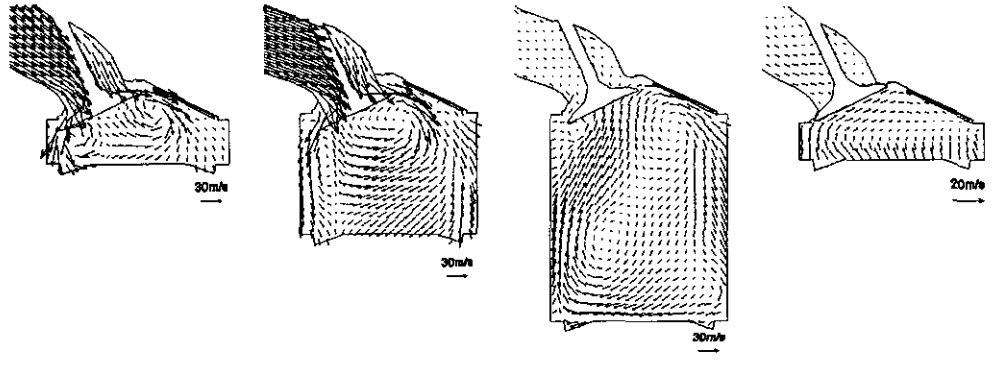

(a) 45° ATDC (a) 90° ATDC (a) BDC (a) 40° BTDC

Fig. 5 Development of flow field during the intake and compression processes (for 35° port)

sion continues, the counterclockwise tumble is diminished and the flow field is characterized by the shrunk clockwise vortices. (Khalighi et al; 1995). Figures 4 and 5 show the flow field by the 15° port and 35° port, respectively. From the comparison of Figs 3, 4, and 5 the overall flow patterns seems to be similar. In Fig. 6, it is found that the 15° port generates most strong tumble flow compared with the others.

Tumble ratio variations are shown in Fig. 6 for

the different port angles. As the intake process starts, the tumble ratio increases sharply due to the increased flow. Near 110° ATDC, the tumble ratio reaches the peak and starts to decrease because of the decreasing flow and friction. However, when a piston moves upwards for compression, the tumble ratio regains its strength since the swirling flow is converted into the tumbling flow. However, after short recovery in the tumble flow, the tumble ratio is gradually decreased again because of friction.

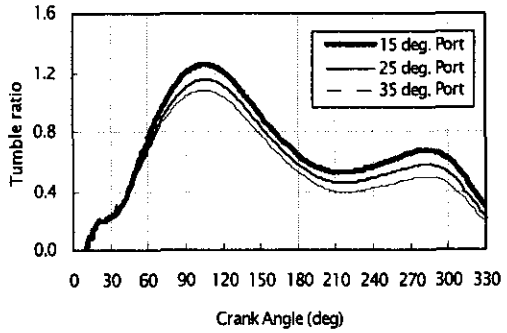

Fig. 6 Tumble ratio variations for the different port angles

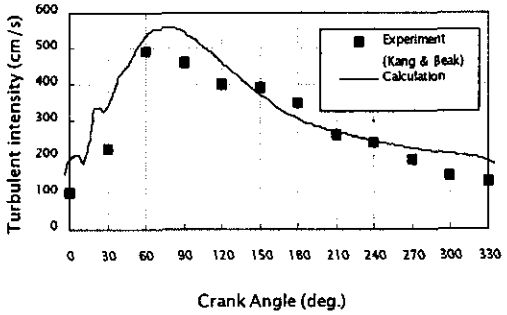

Fig. 7 Turbulent intensity variations for 25° port (at z=8.6 cm)

3.2 Turbulence characteristics

Turbulence plays an important role in combustion. Figure 7 shows the calculated and measured turbulent intensities for 25° port. Turbulent intensity is defined as the magnitude of the fluctuating velocity. Since the turbulence is generated mainly from the jet through valves in the intake process, turbulence intensity reaches a peak when the flow is the maximum. After the peak, turbulence decays in the compression process. Although the calculated values of the turbulent intensity are generally bigger than the experimental values, its trend is satisfactory. The turbulent kinetic energy, TKE, is another useful quantity in assessing the effect of tumbling flow inside a cylinder. The TKE distribution is plotted in Fig. 8 for 25° port. TKE is generated in the intake process and, in the compression process, TKE is decreased drastically because of friction. In Fig. 9, TKE distribution with the different port angles is plotted at 45° BBDC. As expected from the flow field, the 15° port shows high level turbulent kinetic energy regions compared with the other ports. Since high level TKE regions are important for combustion, the 15° port is expected to reveal better combustion characteristics. Figure 10 shows TKE distribution at 40° BTDC, the late stage of the compression process. The 15° port shows wider high TKE regions compared with other ports, although overall magnitude of TKE is decreased significantly.

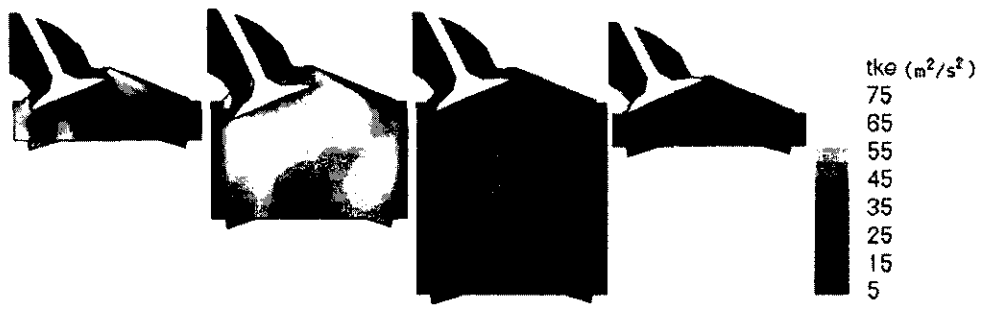

(a) 45° ATDC (b) 90° ATDC (c) BDC (d) 40° BTDC

Fig. 8 Turbulent kinetic energy distributions during the intake and compression processes (for 25° port)

(a) 15° port (b) 25° port (c) 35° port

Fig. 9 Turbulence kinetic energy distributions with the different port angles (at 45° BBDC)

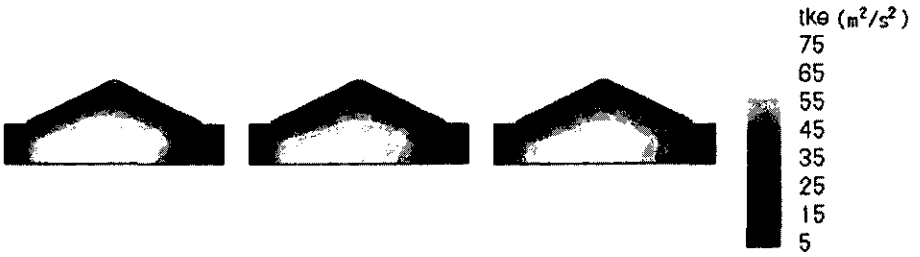

(a) 15° port (b) 25° port (c) 35° port

Fig. 10 Turbulent kinetic energy distributions for the different ports (at 40° BTDC)

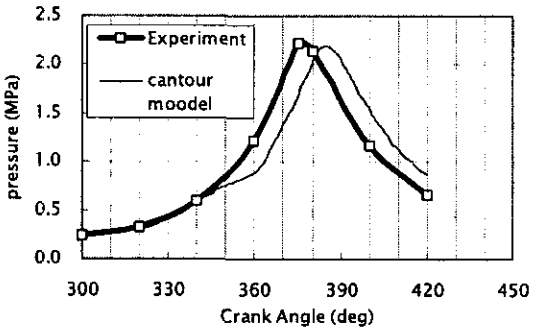

Fig. 11 Cylinder pressure variations during combustion (for 25° port)

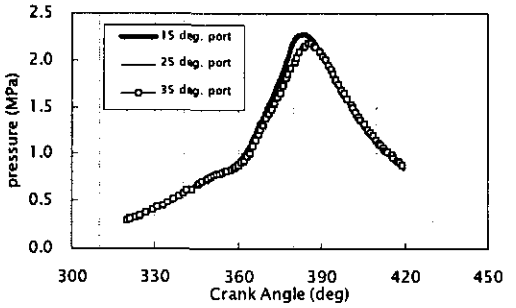

Fig. 12 Cylinder pressure variations during combustion for the different port angles

3.3 Combustion

Figure 11 shows the cylinder pressure variations during the combustion process. The calculated results show the similar results from experiments (Kang et al; 1997), although there is a phase lag. The effect of port configuration on the pressure variation in a cylinder during the combustion process is shown in Fig. 12. As expected in Fig. 10, the 15° port generates a fast pressure rise compared with the others. Figure 13 shows the burned mass fraction of fuel as a function of crank angle for the different intake port angle. The 15° port which has higher turbulence level shows fast burn of the fuel.

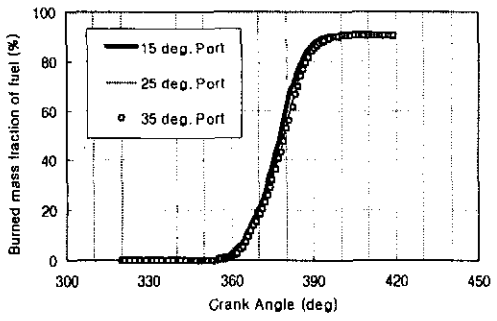

Fig. 13 Burned mass fraction of fuel as a function of crank angle with the different port angles

4. Conclusion

The numerical study on the flow and combustion in a 4 valve engine cylinder was carried out by the KIVA-3V code and the combustion model. The computed velocity profile and cylinder pressure show good agreement with the measurements. From the analysis of the fluid motion inside a cylinder it is found that the intake port angle is the important factor to determine the flow field and the tumble. The 15° port shows the strong tumble flow with high level of turbulence because of smooth passage of the jet flow in the tangential direction. The 35° port shows relatively weak tumble. From the calculation for the combustion process, it is found that high level turbulence is effective in increasing the burning rate. The 15° port shows fast combustion because of high level of turbulence.

Reference

Amsden, A. A., O'Rourke P. J., and Butler, T. D., 1989, "KIVA-Ⅱ: A Computer Program for Chemically Reactive Flows with Sprays," LosAlamos National Laboratory Report No. LA-11560-MS.

Amsden, A. A., 1997, "KIVA-3V: A Block Structured KIVA Program for Engines with Vertical or Canted Valves," LosAlamos National Laboratory Report No. LA-UR-97-698

Cantore, G., Borghi, M., Mattarelli, E. and Bianchi, G. M., 1995, "Numerical Simulation of Turbulent Combustion in a Four Valve Spark Ignition Engine with CRI/TURBOKIVA 2.0 Code," ICE-Vol. 23, Engine Modeling, ASME

Henlot, S., 1989, "Three Dimensional Modeling of Flow and Turbulence in Four-Valve Spark ignition Engine-Comparison with LDV Measurements," SAE Paper 89084.

Jennings, M. J., 1992, "Multi-Dimensional Modeling of Turbulent Premixed Charge Combustion," SAE Paper 920589

Kang K. Y., Lee J. W., Jeong D. S., Jeong S. Y., and Baek J. H., 1994, "The Effect of Intake Port Configurations on the Turbulence Characteristics During Compression Stroke in a Motored Engine," *KSME J.*, Vol. 18, No. 4, pp. 920 ~933.

Kang K. Y. and Baek J. H., 1996, "Tumble Flow and Turbulence Characteristics in a Small Four Valve Engine," SAE paper 960265.

Kang et al., 1997, "Development of Design Techniques for Intake Port and Combustion Chamber," KIMM Technical Report, pp. 301 ~358.

Khalighi, B., El Tahry, S. H., Haworth, D. C. and Huebler, M. S. 1995, "Computation and Measurement of Flow and Combustion in a Four-Valve Engine with Intake Variations," SAE Paper 950287

Magnussen, B. F. and Hjertager, B. H., 1976, "On Mathematical Modeling of Turbulent Combustion with Special Emphasis on Soot Formation and Combustion," *Sixteenth Sym. on Combustion, The Combustion Institute.*

Naitoh, K., 1990, "Numerical Simulation of the Detailed Flow in Engine Ports and Cylinders," SAE Paper 900256.